A Multi-Modal Multi-Objective Evolutionary Algorithm Using Two-Archive and Recombination Strategies
Supplementary Material

Yiping Liu, *Member, IEEE*, Gary G. Yen, *Fellow, IEEE*, and Dunwei Gong, *Member, IEEE*

***Abstract*—There have been few researches on solving multi-modal multi-objective optimization problems, whereas they are commonly seen in real-world applications but difficult for the existing evolutionary optimizers. In this study, we propose a novel multi-modal multi-objective evolutionary algorithm using two-archive and recombination strategies. In the proposed algorithm, the properties of decision variables and the relationships among them are analyzed at first to guide the evolutionary search. Then, a general framework using two archives, i.e., the convergence and the diversity archives, is adopted to cooperatively solve these problems. Moreover, the diversity archive simultaneously employs a clustering strategy to guarantee diversity in the objective space and a niche-based clearing strategy to promote the same in the decision space. At the end of evolution process, the solutions in the convergence and the diversity archives are recombined to obtain a large number of multiple Pareto optimal solutions. In addition, a set of benchmark test functions and a performance metric are designed for multi-modal multi-objective optimization. The proposed algorithm is empirically compared with two state-of-the-art evolutionary algorithms on these test functions. The comparative results demonstrate that the overall performance of the proposed algorithm is significantly superior to the competing algorithms.**

I. Benchmark Test Functions: MMMOP1-6

This is the Supplementary Material of A Multi-Modal Multi-Objective Evolutionary Algorithm Using Two-Archive and Recombination Strategies. Tables I and II give the common properties and the detailed definitions of benchmark test functions proposed in this paper, i.e., MMMOP1-6. Figs. 1-7 shows the Pareto optimal fronts and Pareto optimal solution sets of these problems. Please refer to Subsection IV.A in the main body of the paper for the detailed descriptions of them.

Manuscript received March 9, 2018; revised May 13, 2018 and August 23, 2018; accepted October 28, 2018. This work was jointly supported by National Natural Science Foundation of China with grant No. 61803192, 61876075, 61773384, 61763026, 61673404, 61573361, and 61503220, National Basic Research Program of China (973 Program) with grant No. 2014CB046306-2, National Key R&D Program of China with grant No. 2018YFB1003802-01, and China Scholarship Council with grant No. 201606420005. (*Corresponding author: Gary G. Yen.*)

Y. Liu is with School of Information and Control Engineering, China University of Mining and Technology, Xuzhou 221116, China. (yiping0liu@gmail.com)

G. G. Yen is with the School of Electrical and Computer Engineering, Oklahoma State University, Stillwater, OK 74078, USA. (gyen@okstate.edu)

D. Gong is with School of Information and Control Engineering, China University of Mining and Technology, Xuzhou 221116, China. (dwgong@vip.163.com)

TABLE I
COMMON PROPERTIES OF MMMOP1-6.

	Developed from	Type of Decision Variable	Geometry of PF
MMMOP1	Equal Maxima, DLTZ1	Convergence, Diversity	Linear
MMMOP2	Vincent, DLTZ4	Convergence, Diversity	Concave
MMMOP3	Rastrigin, DLTZ2	Convergence, Diversity	Concave
MMMOP4	Rastrigin, DLTZ3	Convergence, Diversity	Concave
MMMOP5	Rastrigin, DLTZ3	Convergence, Diversity	Concave
MMMOP6	Himmelblau, UF8	Convergence, Mixed	Concave

II. Achieved Solution Sets by Different Algorithms in the Decision Space

We present the achieved solution sets of some representative instances in the decision space by TriMOEA-TA&R, MO_Ring_PSO_SCD [1], and DN-NSGA-II [2] in a given single run to visually investigate their performance in Figs. 8-13. This particular run is associated with the result which is the closest to the mean IGDM value in Table III in the main body of the paper. Readers can compare these achieved solution sets with the PSs in Figs. 2-7 if interested.

III. Investigation on the effect of the recombination strategy in TriMOEA-TA&R

In this section, to investigate the effect of the recombination strategy, we compare TriMOEA-TA&R with its variant, TriMOEA-TA, which does not employ the recombination strategy. That is, in TriMOEA-TA, the diversity archive outputs its solutions as the final solution set, no matter whether the independent convergence-related decision variables are detected or not. The parameter settings of TriMOEA-TA (except the population size set to N_{oth}) are the same as those of TriMOEA-TA&R in Subsection IV.D in the main body of the paper.

All the optimization problems can be classified into three groups.

Group A. For the optimization problems in Group A, there are two or more Pareto optimal solutions which have different independent convergence-related decision variable values for a point on the PF, e.g., A and B types of MMMOP1 and MMMOP2, C and D types of MMMOP3, MMMOP4, MMMOP5, and MMMOP6.

Group B. For the optimization problems in Group B, the Pareto optimal solutions corresponding to each point on the

TABLE II
DEFINITIONS OF MMMOP1-6

MMMOP1	$\min f_1(\boldsymbol{x}) = (1+g(X_A,X_B))x_1x_2\cdots x_{M-1}$ $\min f_2(\boldsymbol{x}) = (1+g(X_A,X_B))x_1x_2\cdots(1-x_{M-1})$ $\vdots$ $\min f_{M-1}(\boldsymbol{x}) = (1+g(X_A,X_B))x_1(1-x_2)$ $\min f_M(\boldsymbol{x}) = (1+g(X_A,X_B))(1-x_1)$ s.t. $\mathrm{x_i} \in [0,1], \mathrm{i}=1,2,...,\mathrm{n}$ with $\mathrm{g(X_A,X_B)} = 100[\mathrm{\lvert X_A\rvert} + \mathrm{\lvert X_B\rvert} - \sum_{\mathrm{x_i}\in\mathrm{X_A}} \sin^6(5\pi \mathrm{x_i}) + \sum_{\mathrm{x_i}\in\mathrm{X_B}} (\mathrm{x_i}-0.5)^2 - \cos(20\pi(\mathrm{x_i}-0.5))]$ Pareto optimal solution: $x_i^* = 0.1, 0.3, 0.5, 0.7,$ or 0.9, for $x_i^* \in X_A$ and $x_i^* = 0.5$, for $x_i^* \in X_B$.
MMMOP2	$\min f_1(\boldsymbol{x}) = (1+g(X_A,X_B))\cos(x_1^\alpha\pi/2)\cdots\cos(x_{M-2}^\alpha\pi/2)\cos(x_{M-1}^\alpha\pi/2)$ $\min f_2(\boldsymbol{x}) = (1+g(X_A,X_B))\cos(x_1^\alpha\pi/2)\cdots\cos(x_{M-2}^\alpha\pi/2)\sin(x_{M-1}^\alpha\pi/2)$ $\vdots$ $\min f_M(\boldsymbol{x}) = (1+g(X_A,X_B))\sin(x_1^\alpha\pi/2)$ s.t. $\mathrm{x_i} \in [0,1], \mathrm{i}=1,2,...,\mathrm{n}$ with $\mathrm{g(X_A,X_B)} = \mathrm{\lvert X_A\rvert} - \sum_{\mathrm{x_i}\in\mathrm{X_A}} \sin(10\log(\mathrm{y_i})) + \sum_{\mathrm{x_i}\in\mathrm{X_B}} (\mathrm{x_i}-0.5)^2$ $y_i = 9.75x_i + 0.25, i = M,...,M+k_A-1$ Pareto optimal solution: $y_i^* = 0.333018, 0.624228, 1.170088, 2.193280, 4.111207,$ or 7.706277, for $x_i^* \in X_A$ and $x_i^* = 0.5$, for $x_i^* \in X_B$.
MMMOP3	$\min f_1(\boldsymbol{x}) = (1+g(X_A,X_B))\cos(y_1\pi/2)\cdots\cos(y_{M-2}\pi/2)\cos(y_{M-1}\pi/2)$ $\min f_2(\boldsymbol{x}) = (1+g(X_A,X_B))\cos(y_1\pi/2)\cdots\cos(y_{M-2}\pi/2)\sin(y_{M-1}\pi/2)$ $\vdots$ $\min f_M(\boldsymbol{x}) = (1+g(X_A,X_B))\sin(y_1\pi/2)$ s.t. $\mathrm{x_i} \in [0,1], \mathrm{i}=1,2,...,\mathrm{n}$ with $\mathrm{g(X_A,X_B)} = \mathrm{\lvert X_A\rvert} + \sum_{\mathrm{x_i}\in\mathrm{X_A}} \cos(2\pi \mathrm{c_i x_i}) + \sum_{\mathrm{x_i}\in\mathrm{X_B}} (\mathrm{x_i}-0.5)^2$ $y_i = x_i d_i - \lfloor x_i d_i \rfloor, i = 1,2,...,M-1$ where $d_i > 0, i = 1,...,M-1$ is integer, and $c_i > 1, i = M,...,M+k_A-1$ is integer. Pareto optimal solution: $x_i^* = \frac{1}{2c_i}, \frac{3}{2c_i}, ...,$ or $\frac{2c_i-1}{2c_i}$, for $x_i^* \in X_A$ and $x_i^* = 0.5$, for $x_i^* \in X_B$.
MMMOP4	$\min f_1(\boldsymbol{x}) = (1+g(X_A,X_B))\cos(y_1\pi/2)\cdots\cos(y_{M-2}\pi/2)\cos(y_{M-1}\pi/2)$ $\min f_2(\boldsymbol{x}) = (1+g(X_A,X_B))\cos(y_1\pi/2)\cdots\cos(y_{M-2}\pi/2)\sin(y_{M-1}\pi/2)$ $\vdots$ $\min f_M(\boldsymbol{x}) = (1+g(X_A,X_B))\sin(y_1\pi/2)$ s.t. $\mathrm{x_i} \in [0,1], \mathrm{i}=1,2,...,\mathrm{n}$ with $\mathrm{g(X_A,X_B)} = 100[\mathrm{\lvert X_A\rvert} + \mathrm{\lvert X_B\rvert} + \sum_{\mathrm{x_i}\in\mathrm{X_A}} \cos(2\pi \mathrm{c_i x_i}) + \sum_{\mathrm{x_i}\in\mathrm{X_B}} (\mathrm{x_i}-0.5)^2 - \cos(20\pi(\mathrm{x_i}-0.5))]$ $y_i = \begin{cases} x_i d_{\text{sum}}/d_i, \text{if } x_i d_{\text{sum}} \le d_i \\ (x_i d_{\text{sum}} - d_i)/d_i, \text{if } d_i < x_i d_{\text{sum}} \le d_i + d_i - 1 \\ (x_i d_{\text{sum}} - d_i - (d_i-1))/d_i, \text{if } d_i + d_i - 1 < x_i d_{\text{sum}} \le d_i + d_i - 1 + d_i - 2 \\ \vdots \\ (x_i d_{\text{sum}} - (d_{\text{sum}}-1))/d_i, \text{if } d_{\text{sum}} - 1 < x_i d_{\text{sum}} \end{cases}, i = 1,2,...,M-1$ $d_{\text{sum}} = d_i(d_i+1)/2$ where $d_i > 0, i = 1,...,M-1$ is integer, and $c_i > 1, i = M,...,M+k_A-1$ is integer. Pareto optimal solution: $x_i^* = \frac{1}{2c_i}, \frac{3}{2c_i}, ...,$ or $\frac{2c_i-1}{2c_i}$, for $x_i^* \in X_A$ and $x_i^* = 0.5$, for $x_i^* \in X_B$.
MMMOP5	$\min f_1(\boldsymbol{x}) = (1+g(X_A,X_B))\cos(y_1\pi/2)\cdots\cos(y_{M-2}\pi/2)\cos(y_{M-1}\pi/2)$ $\min f_2(\boldsymbol{x}) = (1+g(X_A,X_B))\cos(y_1\pi/2)\cdots\cos(y_{M-2}\pi/2)\sin(y_{M-1}\pi/2)$ $\vdots$ $\min f_M(\boldsymbol{x}) = (1+g(X_A,X_B))\sin(y_1\pi/2)$ s.t. $\mathrm{x_i} \in [0,1], \mathrm{i}=1,2,...,\mathrm{n}$ with $\mathrm{g(X_A,X_B)} = 100[\mathrm{\lvert X_A\rvert} + \mathrm{\lvert X_B\rvert} + \sum_{\mathrm{x_i}\in\mathrm{X_A}} \cos(2\pi \mathrm{c_i x_i}) + \sum_{\mathrm{x_i}\in\mathrm{X_B}} (\mathrm{x_i}-0.5)^2 - \cos(20\pi(\mathrm{x_i}-0.5))]$ $y_i = \begin{cases} x_i d_{\text{sum}}/2^{d_i}, \text{if } x_i d_{\text{sum}} \le 2^{d_i} \\ (x_i d_{\text{sum}} - 2^{d_i})/2^{d_i-1}, \text{if } 2^{d_i} < x_i d_{\text{sum}} \le 2^{d_i} + 2^{d_i-1} \\ (x_i d_{\text{sum}} - 2^{d_i} - 2^{d_i-1})/2^{d_i-2}, \text{if } 2^{d_i} + 2^{d_i-1} < x_i d_{\text{sum}} \le 2^{d_i} + 2^{d_i-1} + 2^{d_i-2} \\ \vdots \\ (x_i d_{\text{sum}} - (d_{\text{sum}}-1))/2^0, \text{if } d_{\text{sum}} - 1 < x_i d_{\text{sum}} \end{cases}, i = 1,2,...,M-1$ $d_{\text{sum}} = 2^{d_i+1} - 1$ where $d_i > 0, i = 1,...,M-1$ is integer, and $c_i > 1, i = M,...,M+k_A-1$ is integer. Pareto optimal solution: $x_i^* = \frac{1}{2c_i}, \frac{3}{2c_i}, ...,$ or $\frac{2c_i-1}{2c_i}$, for $x_i^* \in X_A$ and $x_i^* = 0.5$, for $x_i^* \in X_B$.
MMMOP6	$\min f_1(\boldsymbol{x}) = g(X_A,X_B) + \cos(x_1\pi/2)\cdots\cos(x_{M-2}\pi/2)\cos(x_{M-1}\pi/2)$ $\min f_2(\boldsymbol{x}) = g(X_A,X_B) + \cos(x_1\pi/2)\cdots\cos(x_{M-2}\pi/2)\sin(x_{M-1}\pi/2)$ $\vdots$ $\min f_M(\boldsymbol{x}) = g(X_A,X_B) + \sin(x_1\pi/2)$ s.t. $\mathrm{x_i} \in [0,1], \mathrm{i}=1,2,...,\mathrm{n}$ with $\mathrm{g(X_A,X_B)} = \sum_{\mathrm{i}=\mathrm{M},\mathrm{M+2},...,\mathrm{M+k_A-2}} [(\mathrm{y_i^2} + \mathrm{y_{i+1}} - 11)^2 + (\mathrm{y_i} + \mathrm{y_{i+1}^2} - 7)^2] + \sum_{\mathrm{x_i}\in\mathrm{X_B}} (\mathrm{z_i} - \mathrm{t_i})^2$ $y_i = 12(x_i - 0.5), i = M,...,M+k_A-1$ $z_i = 2c_i x_i - 2\lfloor c_i x_i \rfloor - 1, i = M+k_A,...,n$ $t_i = \prod_{j=1,...,M-1} sin(2\pi x_j + \frac{(i-M-k_A)\pi}{k_B}), i = M+k_A,...,n$ where $c_i > 0, i = M+k_A,...,n$ is integer. k_A must be even in MMMOP6. Pareto optimal solution: $(y_i^*, y_{i+1}^*) = (3.0, 2.0)$ or $(-2.80511, 3.13131)$ or $(-3.77931, -3.28318)$ or $(3.58442, -1.84812)$, for $x_i^* \in X_A$ and $z_i^* = t_i^*$, for $x_i^* \in X_B$.

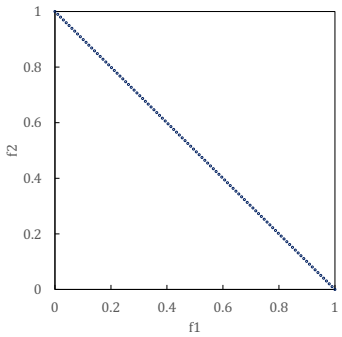

(a) MMMOP1 ($M = 2$)

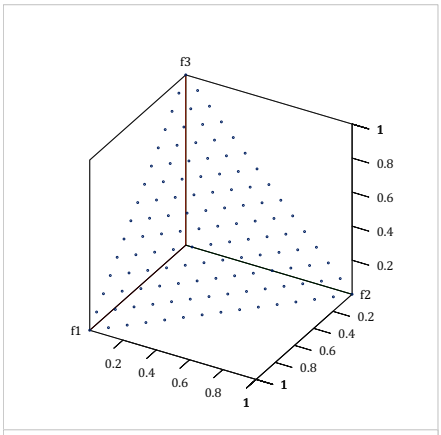

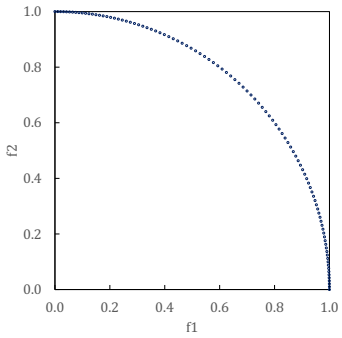

(c) MMMOP2-6 ($M = 2$)

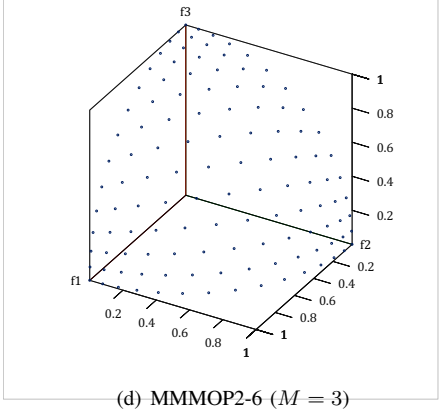

(d) MMMOP2-6 ($M = 3$)

Fig. 1. PFs of MMMOP1-6.

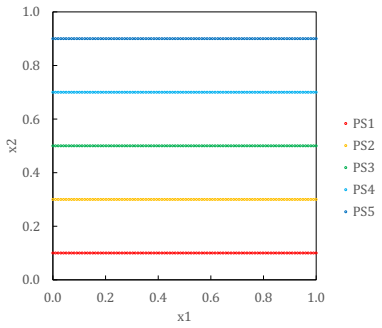

Fig. 2. PS of MMMOP1 with $M = 2$ and $k_A = 1$. Each of the five lines (i.e. $PS_1, ..., PS_5$) can be mapped to the whole PF.

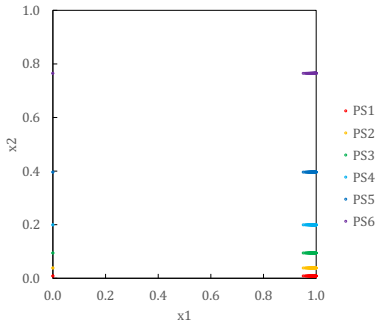

Fig. 3. PS of MMMOP2 with $M = 2$ and $k_A = 1$. Each of the six lines (i.e. $PS_1, ..., PS_6$) can be mapped to the whole PF.

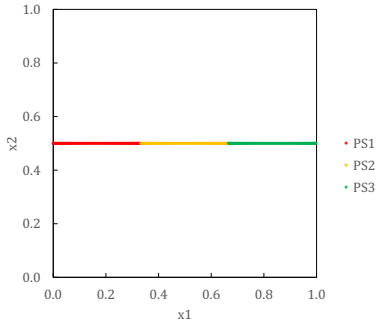

(a) $M = 2, k_A = 0, d_1 = 3$

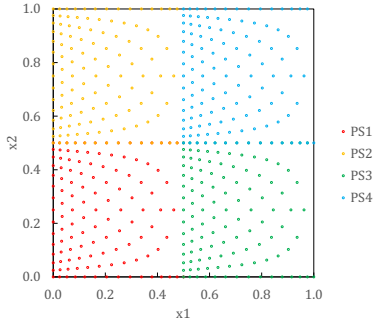

(b) $M = 3, d_1 = 2, d_2 = 2$

Fig. 4. PSs of MMMOP3. Each optimal region (e.g., $PS_1, PS_2, ...$) can be mapped to the whole PF.

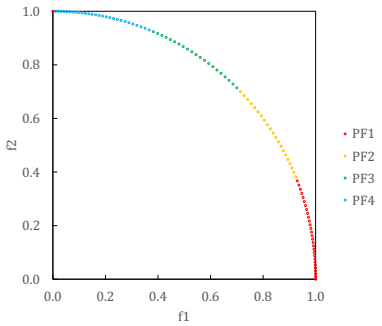

(a) PF

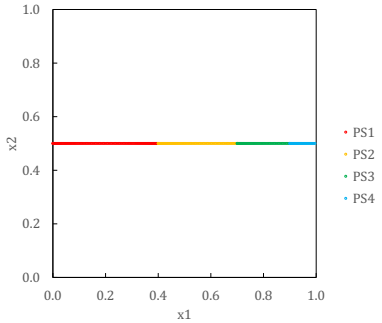

(b) PS

Fig. 5. PF and PS of MMMOP4 ($M = 2, k_A = 0, d_1 = 4$). PS_4 can be mapped to the whole Pareto front, whereas PS_2 can only be mapped to $PF_2 \cup PF_3 \cup PF_4$, PS_3 to $PF_3 \cup PF_4$, and PS_4 to PF_4. Consequently, each point on PF_1, PF_2, PF_3, and PF_4 is corresponded to 4, 3, 2, and 1 Pareto optimal solution(s), respectively.

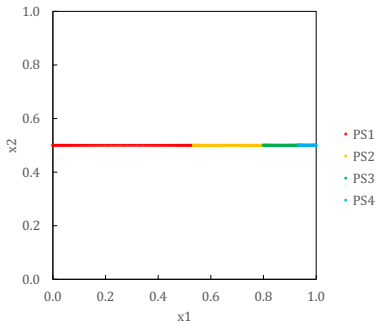

(a) $M = 2, k_A = 0, d_1 = 3$

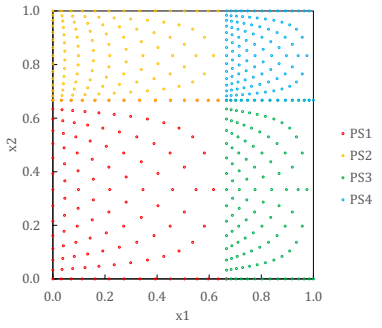

(b) $M = 3, d_1 = 1, d_2 = 1$

Fig. 6. PSs of MMMOP5. Each optimal region (e.g., PF_1,PF_2,...) can be mapped to the whole PF. However, they have different spaces.

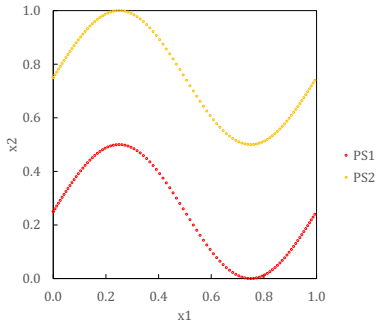

(a) $M = 2, k_A = 0, c_1 = 2$

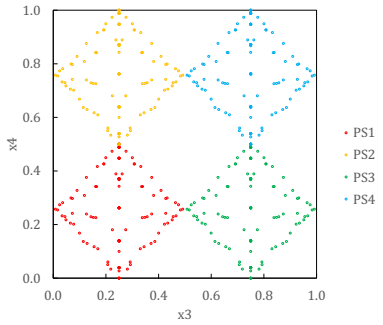

(b) $M = 3, k_A = 0, c_1 = 2, c_2 = 2$

Fig. 7. PSs of MMMOP6. Each optimal region (e.g., PF_1,PF_2,...) can be mapped to the whole PF.

PF have the same independent convergence-related decision variable values, e.g., A and B types of MMMOP3, MMMOP4, MMMOP5.

Group C. The optimization problems in Group C have no independent convergence-related decision variable, e.g., A and B types of MMMOP6, and MMF1-8.

In Table III, we show the results of IGDM, GD [3], and runtime obtained by TriMOEA-TA&R and TriMOEA-TA on Group A and B. We do not show the results on Group C, since TriMOEA-TA&R does not employ the recombination strategy when the independent convergence-related decision variables are not detected by the decision variable analytical technique. In this situation, TriMOEA-TA&R and TriMOEA-TA behave exactly the same. In Table III, '+' ('−') indicates that TriMOEA-TA&R shows significantly better (worse) performance than TriMOEA-TA. '=' indicates that there is no significant difference between the compared results.

From Table III, we can see that TriMOEA-TA&R significantly outperforms TriMOEA-TA on most test problems in Group A according to IGDM. However, TriMOEA-TA&R achieves a worse IGDM value than TriMOEA-TA on MMMOP2-B. The reason is that the improper setting of σ_{niche} results in missing peak solutions in the convergence archive, which considerably reduces the TriMOEA-TA&R's ability in obtaining all the parts of PS on MMMOP2-B. On the other hand, TriMOEA-TA does not count on the peak solutions, since it does not employ the recombination strategy. According to the results of GD and runtime, TriMOEA-TA&R has significant better convergence performance and runs faster than TriMOEA-TA on all test problems in Group A.

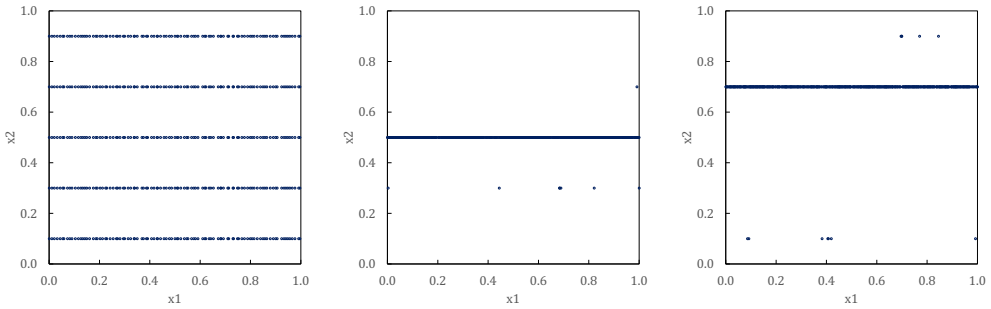

(a) MMMOP1-A by TriMOEA-TA&R (b) MMMOP1-A by MO_Ring_PSO_SCD (c) MMMOP1-A by DN-NSGA-II

Fig. 8. Achieved solution sets of MMMOP1-A by different algorithms.

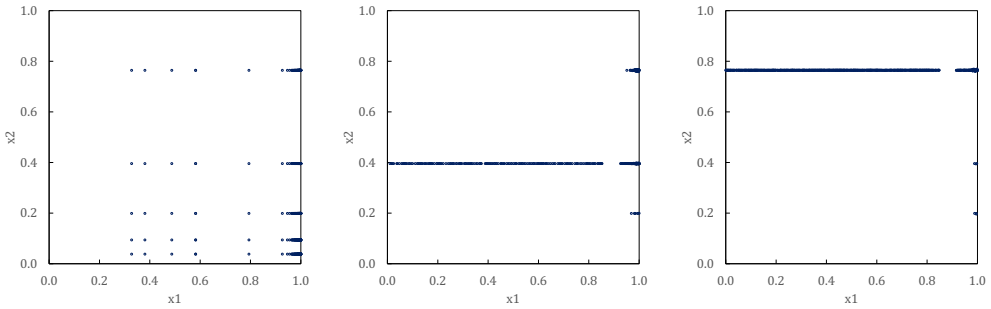

(a) MMMOP2-A by TriMOEA-TA&R (b) MMMOP2-A by MO_Ring_PSO_SCD (c) MMMOP2-A by DN-NSGA-II

Fig. 9. Achieved solution sets of MMMOP2-A by different algorithms.

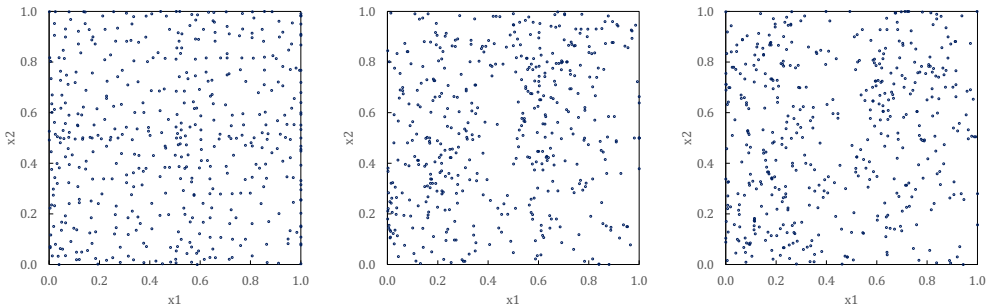

(a) MMMOP3-B by TriMOEA-TA&R (b) MMMOP3-B by MO_Ring_PSO_SCD (c) MMMOP3-B by DN-NSGA-II

Fig. 10. Achieved solution sets of MMMOP3-B by different algorithms.

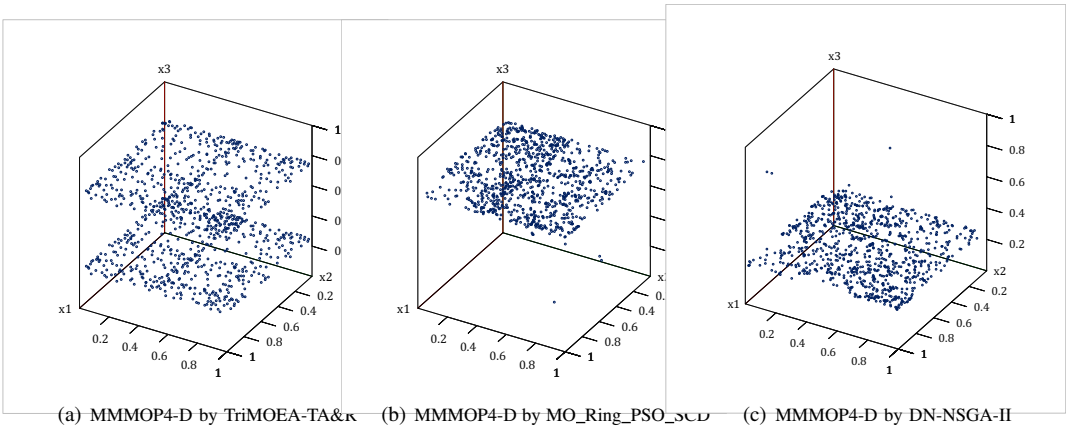

(a) MMMOP4-D by TriMOEA-TA&R (b) MMMOP4-D by MO_Ring_PSO_SCD (c) MMMOP4-D by DN-NSGA-II

Fig. 11. Achieved solution sets of MMMOP4-D by different algorithms.

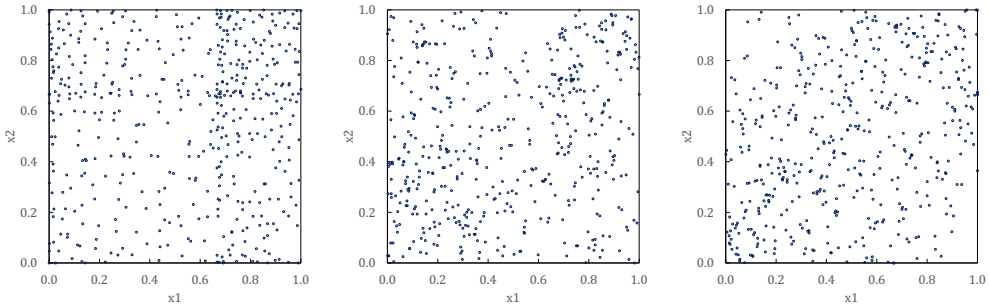

(a) MMMOP5-B by TriMOEA-TA&R (b) MMMOP5-B by MO_Ring_PSO_SCD (c) MMMOP5-B by DN-NSGA-II

Fig. 12. Achieved solution sets of MMMOP5-B by different algorithms.

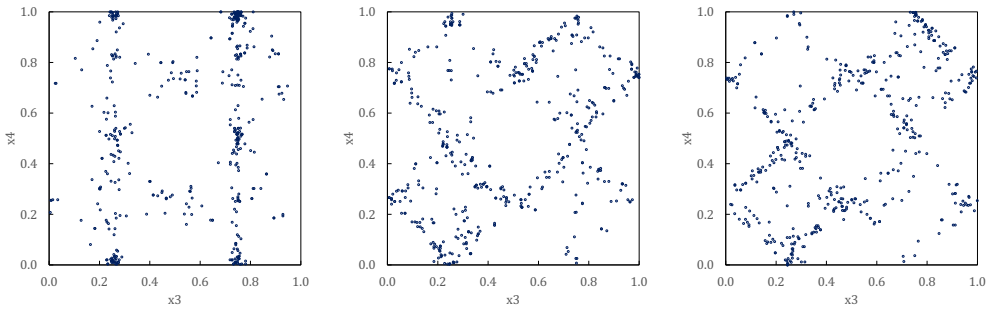

(a) MMMOP6-B by TriMOEA-TA&R (b) MMMOP6-B by MO_Ring_PSO_SCD (c) MMMOP6-B by DN-NSGA-II

Fig. 13. Achieved solution sets of MMMOP6-B by different algorithms.

TABLE III
COMPARISON BETWEEN TRIMOEA-TA&R AND TRIMOEA-TA

	TriMOEA-TA&R	TriMOEA-TA	TriMOEA-TA&R	TriMOEA-TA	TriMOEA-TA&R	TriMOEA-TA
Group A	IGDM		GD		Runtime (Unit: Sec)	
MMMOP1-A	**4.200E-3**	+ 2.632E-1	**3.500E-5**	+ 4.364E-3	**2.684E+0**	+ 4.522E+1
MMMOP1-B	**7.961E-2**	+ 2.839E-1	**1.257E-3**	+ 1.139E-1	**3.093E+0**	+ 6.760E+1
MMMOP2-A	**1.377E-1**	+ 3.739E-1	**1.626E-3**	+ 3.750E-3	**2.646E+0**	+ 6.531E+1
MMMOP2-B	3.732E-1	- **2.735E-1**	**3.504E-3**	+ 3.956E-3	**3.504E+0**	+ 9.721E+1
MMMOP3-C	**1.718E-2**	= 2.209E-1	**4.318E-4**	+ 3.160E-3	**6.607E+0**	+ 1.100E+2
MMMOP3-D	**5.865E-2**	= 5.471E-2	**4.564E-4**	+ 3.763E-3	**1.354E+1**	+ 1.337E+2
MMMOP4-C	**3.251E-2**	+ 4.289E-1	**9.730E-4**	+ 3.620E-3	**8.646E+0**	+ 4.485E+1
MMMOP4-D	**5.833E-2**	+ 1.545E-1	**1.343E-3**	+ 5.945E-2	**1.283E+1**	+ 1.004E+2
MMMOP5-C	**1.076E-1**	+ 4.774E-1	**1.403E-3**	+ 5.542E-2	**7.009E+0**	+ 3.976E+1
MMMOP5-D	**5.250E-2**	+ 2.132E-1	**1.704E-3**	+ 7.965E-3	**1.297E+1**	+ 1.226E+2
MMMOP6-C	**2.544E-1**	+ 7.405E-1	**2.173E-4**	+ 3.540E-4	**7.131E+0**	+ 2.506E+1
MMMOP6-D	**1.347E-1**	+ 4.527E-1	**5.685E-3**	+ 2.764E-2	**3.187E+1**	+ 1.586E+2
Group B	IGDM		GD		Runtime (Unit: Sec)	
MMMOP3-A	**5.125E-3**	= 5.232E-3	**0.000E+0**	+ 1.480E-4	6.767E+0	= **6.678E+0**
MMMOP3-B	**5.411E-2**	+ 5.661E-2	**2.000E-5**	+ 5.169E-3	6.895E+1	= **5.005E+1**
MMMOP4-A	**5.311E-3**	= 5.332E-3	**6.080E-7**	+ 8.478E-3	**9.323E+0**	= 9.678E+0
MMMOP4-B	6.022E-2	= **5.920E-2**	**2.492E-3**	+ 6.063E-3	**1.496E+1**	= 1.523E+1
MMMOP5-A	**4.925E-3**	+ 6.689E-3	**0.000E+0**	+ 3.789E-3	**1.261E+1**	= 1.307E+1
MMMOP5-B	5.325E-2	= **5.314E-2**	**2.088E-3**	+ 3.541E-2	**1.450E+1**	= 1.520E+1

For the test problems in Group B, TriMOEA-TA&R significantly performs better than TriMOEA-TA only on MMMOP3-B and MMMOP5-A according to IGDM. However, it obtains significantly better GD values on all test problems. The two algorithms do not show significant difference on runtime.

From the above observations, we can conclude that for TriMOEA-TA&R, (1) the recombination strategy can improve the convergence performance and reduce the computational cost for the optimization problems in Group A; (2) the recombination strategy can improve the convergence performance for the optimization problems in Group B; and (3) the recombination strategy will not incur additional computational expense for the optimization problems in Group C, since it will not be employed for these problems.

IV. SENSITIVITY ANALYSES OF THE PARAMETERS IN TRIMOEA-TA&R

In this section, we examine the effects of σ_{niche} and p_{con} on the behavior of TriMOEA-TA&R. The parameter settings in this section are the same as those in the Subsection IV.D in the main body of the paper if they are not expressly stated.

A. Effect of Parameter σ_{niche} on Finding Peak Solutions

Finding all the peak solutions is very important for TriMOEA-TA&R. In this subsection, the effect of parameter σ_{niche} on finding peak solutions in the convergence archive is investigated. MMMOP1-B is chosen as an example. Note that similar results can also be obtained on other test instances. Fig. 14 shows the average number of peak solutions w.r.t. σ_{niche} achieved in the convergence archive on MMMOP1-B in 30 runs. In these 30 runs, p_{con} is set to 1. This means that only the convergence archive is active for evolution. Since there are five Pareto optimal solutions which have different independent convergence-related decision variable values for each point on the PF of MMMOP1-B, it is best to find five peak solutions in the convergence archive.

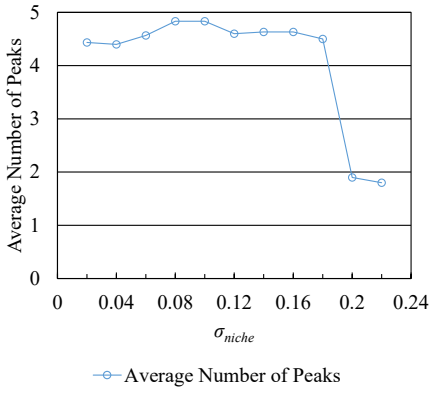

Fig. 14. The average number of peak solutions w.r.t. σ_{niche} achieved in the convergence archive on MMMOP1-B.

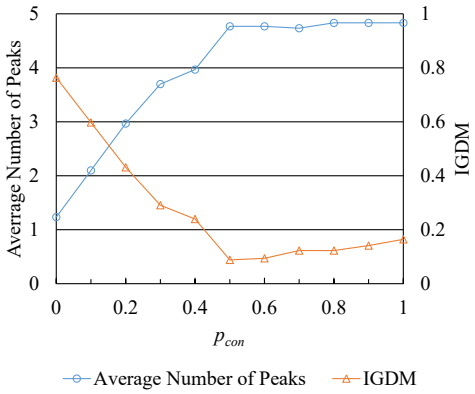

Fig. 15. The average number of peak solutions and IGDM w.r.t. p_{con} achieved in the convergence archive on MMMOP1-B.

We can see from Fig. 14 that as σ_{niche} increases from 0.02 to 0.08, the convergence archive can find more peak solutions. This indicates that a large value of σ_{niche} can increase the ability of the convergence archive in finding peak solution. However, when σ_{niche} is larger than 0.1, the average number of peak solutions declines. Particularly, the average number of peak solutions declines falls rapidly when $\sigma_{niche} \geq 0.2$. The reason is that the distance between two different closest Pareto optimal solutions in the independent convergence-related decision space is 0.2 in MMMOP1-B. This suggests that too much large value of σ_{niche} will result in missing peak solutions. Therefore, for a given MMMOP, we need to set σ_{niche} to a proper value to find all the peak solution. Similarly, for the diversity maintenance in the diversity archive, σ_{niche} should also be tuned to achieve the best performance.

B. Effect of Parameter p_{con} on Finding Peak Solutions

We investigate the effect of parameter p_{con} on finding peak solutions in this subsection. MMMOP1-B is chosen as an example and similar results can also be obtained on other test instances. Fig. 15 shows the average number of peak solutions and IGDM w.r.t. p_{con} obtained on MMMOP1-B in 30 runs. $p_{con} = 0$ indicates that only the diversity archive is active for evolution.

From Fig. 15, we can see that as p_{con} increases, the average number of peak solutions increases, and it becomes flat when $p_{con} > 0.5$. When $p_{con} < 0.5$, the value of IGDM decreases rapidly. However, it increases when $p_{con} > 0.5$. The reason is that when $p_{con} < 0.5$, the larger value of p_{con}, the larger number of peak solutions are found. Then more non-dominated solutions can be achieved by the recombination strategy and a better IGDM value can be obtained. When $p_{con} > 0.5$, almost all the peak solutions can be found, and a large value of p_{con} will decrease the ability of the diversity archive in promoting diversity. Thus the value of IGDM increases as p_{con} increases. Therefore, we recommend to set p_{con} to 0.5 to balance the searching requirements from the convergence and the diversity archives.

C. Effect of Parameter p_{con} on Converging

The effect of parameter p_{con} on converging is examined in this subsection. We chose MMMOP3-B and MMMOP3-E as examples. In MMMOP3-E, $M = 6, k_A = 0, k_B = 5, d_1 = d_2 = 2, d_3 = d_4 = d_5 = 1$. To avoid the possible effect of the recombination strategy, TriMOEA-TA is adopted in this subsection. When solving MMMOP3-E, the population size is set to 528, σ_{niche} is set to 0.3, and the size of F^* is set to 1308 for calculating IGDM. Figs. 16 and 17 shows the curves of GD and IGD w.r.t. generations obtained by TriMOEA-TA on MMMOP3-B and MMMOP3-E when $p_{con} = 0, 0.2, 0.4, 0.6, 0.8, 1$, respectively. Since the algorithm has almost converged after about 100 generations, we only show the curves before 200 generations.

We can see from Figs. 16 and 17 that in general, the larger value of p_{con}, the smaller value of GD and the faster convergence rate. This phenomenon is more obvious on MMMOP3-E, since MMMOP3-E is a many-objective optimization problem [4] and it is more difficult to obtain solutions that close to the PF. This suggests that the convergence archive with a large value of p_{con} can promote the convergence performance a lot. On the other hand, we can observe that a too large value of p_{con} results in a large value of IGDM. Particularly, the value of IGDM increases with generations when $p_{con} = 1$ after the first several generations. The reason is that the diversity archive fails to maintain diversity under this setting. Therefore, without the recombination strategy, we recommend to set p_{con} to 0.2 to get a good overall performance.

D. Ranks in the archives

To investigate why the convergence archive can improve the convergence performance, we show the percentages of candidate solutions with different ranks in the two archives when solving MMMOP3-E with σ_{niche} set to 0.3 and the population size set to 528, 792, and 1056, respectively, in Fig. 18. We also show the results with the population size set to 528 and the σ_{niche} set to 0.1, 0.2, 0.4, and 0.5, respectively. The first four ranks and the remainder solutions are shown in different colors.

From Fig. 18, we can see that in all cases of the diversity archive, i.e., (a), (b), and (c), the percentage of solutions in the first rank grows quickly in the first few generations,

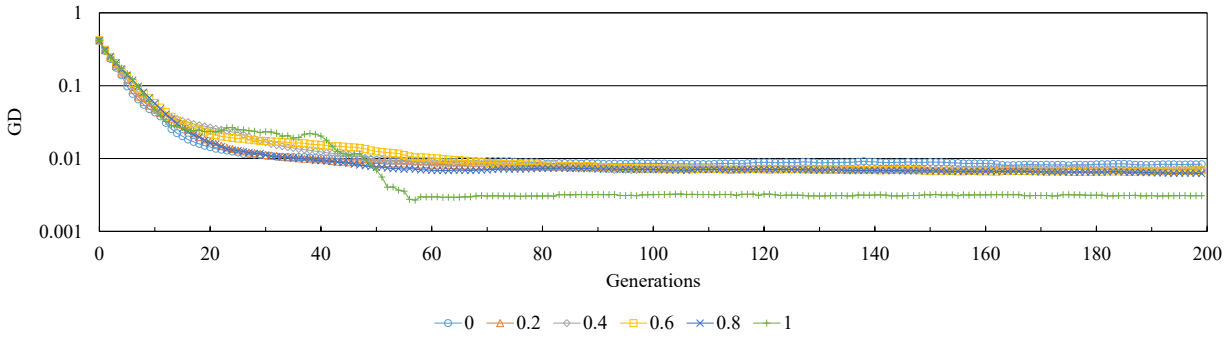

(a) GD

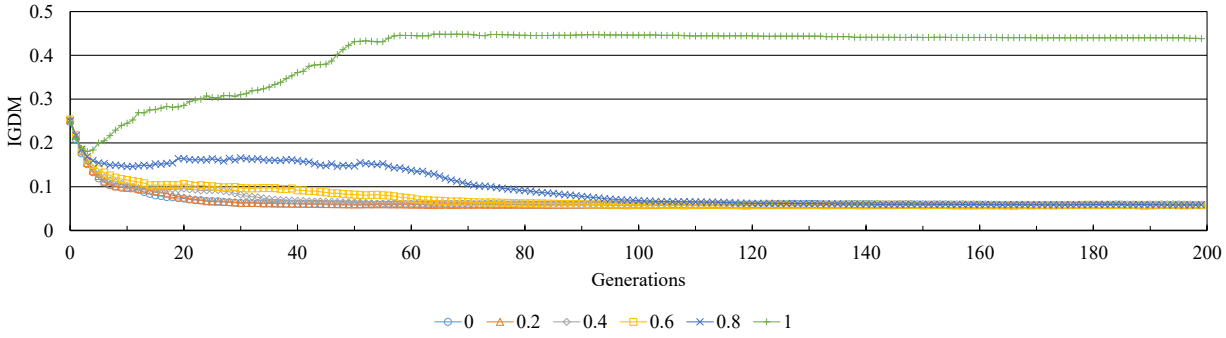

(b) IGDM

Fig. 16. The curves of GD and IGD w.r.t. generations obtained by TriMOEA-TA on MMMOP3-B when $p_{con} = 0, 0.2, 0.4, 0.6, 0.8, 1$.

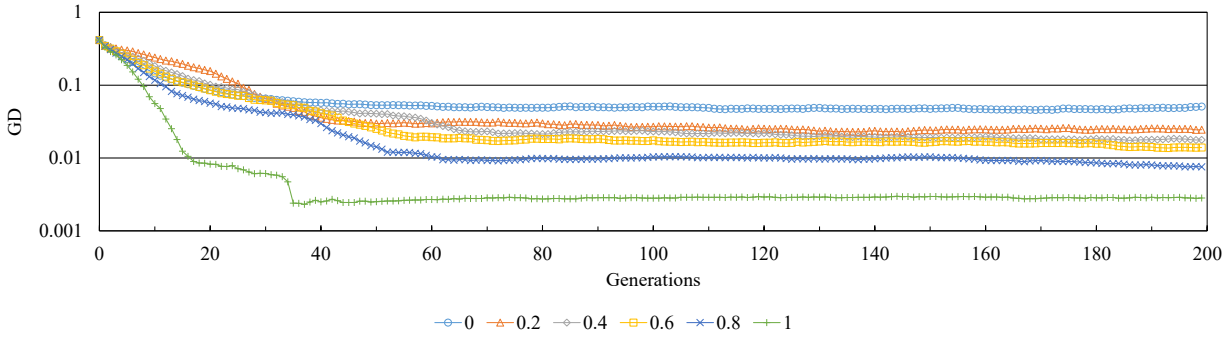

(a) GD

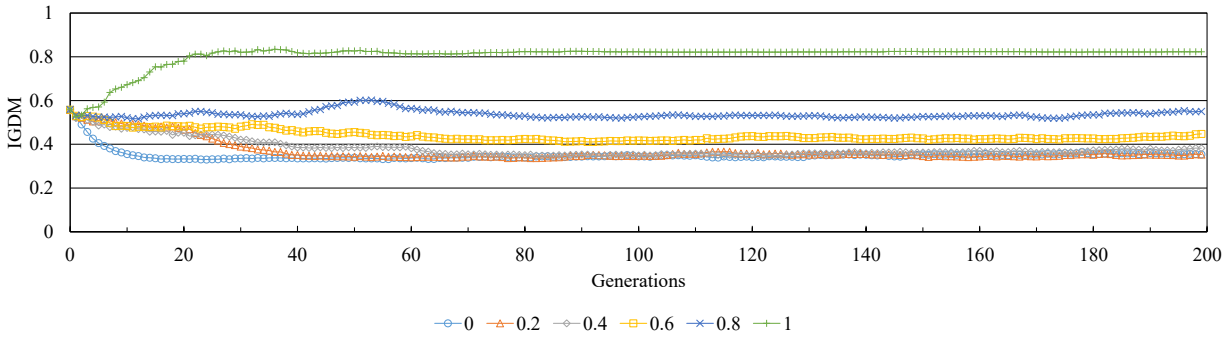

(b) IGDM

Fig. 17. The curves of GD and IGD w.r.t. generations obtained by TriMOEA-TA on MMMOP3-E when $p_{con} = 0, 0.2, 0.4, 0.6, 0.8, 1$.

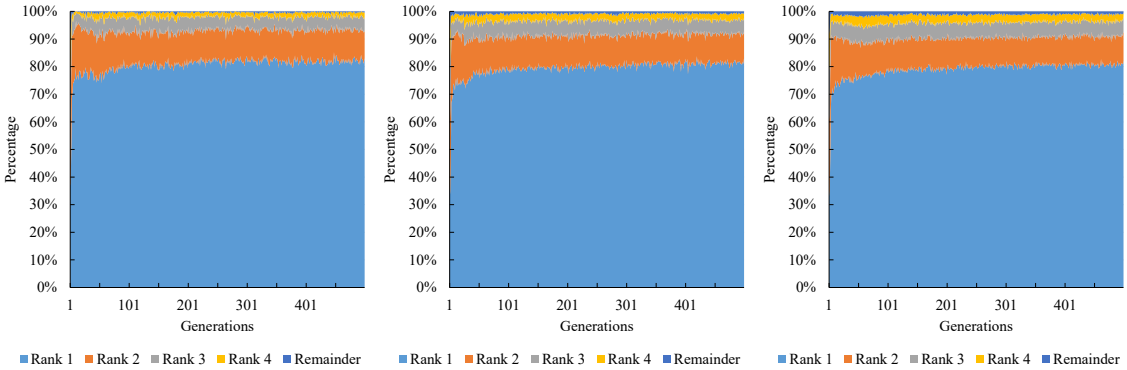

(a) $A_D(N = 528, \sigma_{niche} = 0.3)$ (b) $A_D(N = 792, \sigma_{niche} = 0.3))$ (c) $A_D(N = 1056, \sigma_{niche} = 0.3)$

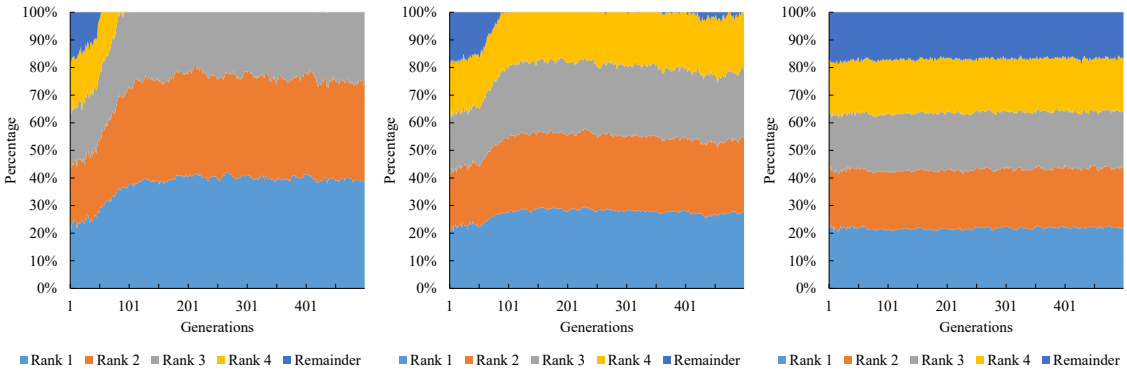

(d) $A_C(N = 528, \sigma_{niche} = 0.3)$ (e) $A_C(N = 792, \sigma_{niche} = 0.3)$ (f) $A_C(N = 1056, \sigma_{niche} = 0.3)$

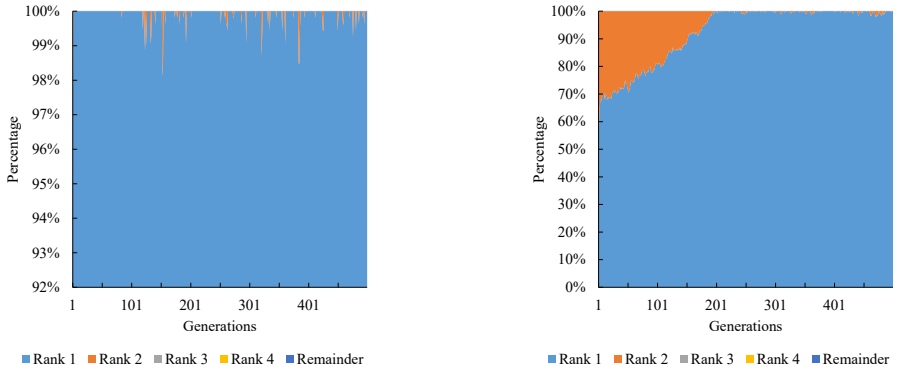

(g) $A_C(N = 528, \sigma_{niche} = 0.1)$ (h) $A_C(N = 528, \sigma_{niche} = 0.2)$

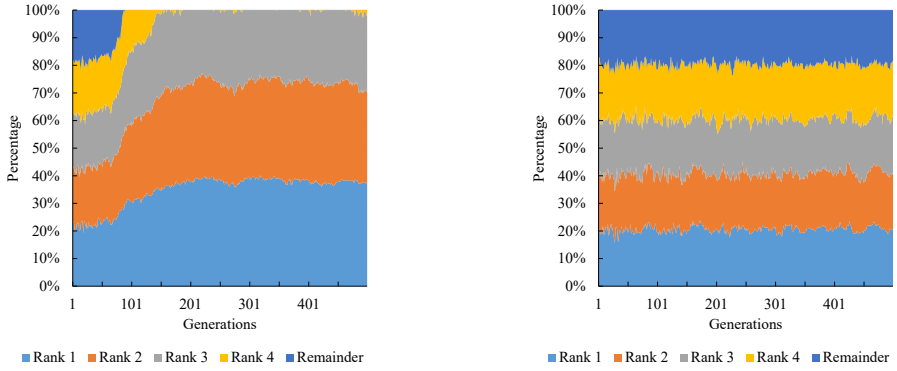

(i) $A_C(N = 528, \sigma_{niche} = 0.4)$ (j) $A_C(N = 528, \sigma_{niche} = 0.5)$

Fig. 18. The percentages of ranks in the convergence and the diversity archives.

TABLE IV
RESULTS OF PSP

PSP	TriMOEA-TA&R	MO_Ring_PSO_SCD		DN-NSGA-II	
MMMOP1-A	**3.960E+02**	7.511E+00	+	8.179E-01	+
MMMOP1-B	**2.052E+01**	2.590E+00	+	1.982E+00	+
MMMOP2-A	2.213E+01	**4.682E+01**	-	1.252E+00	+
MMMOP2-B	**3.620E+01**	4.092E+00	+	3.058E+00	+
MMMOP3-A	**1.189E+03**	1.399E+02	+	1.101E+02	+
MMMOP3-B	**2.967E+01**	6.105E+00	+	5.071E+00	+
MMMOP3-C	**8.349E+02**	9.849E+00	+	1.854E+00	+
MMMOP3-D	**5.267E+01**	5.764E+00	+	4.415E+00	+
MMMOP4-A	**9.942E+02**	2.628E+02	+	8.018E+02	+
MMMOP4-B	**5.072E+01**	2.554E+00	+	2.309E+00	+
MMMOP4-C	**9.399E+02**	2.657E+00	+	1.725E+00	+
MMMOP4-D	**5.061E+01**	2.740E+00	+	2.210E+00	+
MMMOP5-A	**1.351E+03**	2.994E+02	+	9.937E+02	+
MMMOP5-B	**5.601E+01**	2.748E+00	+	2.474E+00	+
MMMOP5-C	**8.837E+02**	2.992E+00	+	1.467E+00	+
MMMOP5-D	**5.599E+01**	2.887E+00	+	2.333E+00	+
MMMOP6-A	**2.157E+02**	1.179E+02	+	2.772E+01	+
MMMOP6-B	**1.556E+01**	1.274E+01	+	4.178E+00	+
MMMOP6-C	**8.831E+00**	5.786E+00	+	1.277E+00	+
MMMOP6-D	**1.586E+01**	5.582E+00	+	2.903E+00	+
Sumup of MMMOP	+ \ - \ =	19 \ 1 \ 0		20 \ 0 \ 0	
MMF1	1.127E+02	**1.362E+02**	-	9.378E+01	+
MMF2	1.075E+02	**1.116E+02**	=	6.941E+01	=
MMF3	3.752E+01	**4.693E+01**	-	3.058E+01	+
MMF4	**3.286E+02**	2.356E+02	+	7.651E+01	+
MMF5	1.100E+02	**1.212E+02**	-	4.026E+01	+
MMF6	**1.044E+02**	1.011E+02	=	4.283E+01	+
MMF7	**2.612E+02**	2.194E+02	+	1.936E+02	+
MMF8	6.096E+01	**3.466E+02**	-	1.316E+02	-
Sumup of MMF	+ \ - \ =	2 \ 4 \ 2		6 \ 1 \ 1	
Sumup of All	+ \ - \ =	21 \ 5 \ 2		26 \ 1 \ 1	

and then remains at more than 70%. Since only 50% of the candidate solutions can be selected into the next generation, the selected ones in the diversity archive are usually in the first rank. This implies that the diversity archive has difficulty in distinguishing solutions with good convergence. On the other hand, when setting σ_{niche} to 0.3 in the convergence archive, the percentage of solutions in the first rank goes down below 50% in all the cases, i.e., (d), (e), and (f). As the population size increases, the solutions are assigned into more ranks. The reason is that σ_{niche} is fixed in (d), (e), and (f). However, if σ_{niche} is set too small, e.g., 0.1 or 0.2 in (g) or (h), the solutions in the convergence archive are almost in the same rank. Conversely, we can see from (i) and (j) that a larger σ_{niche} results in more ranks. This suggests that σ_{niche} should not be set at a very small value, so that the convergence archive has a good ability in selecting solutions with good convergence.

V. COMPARISON AMONG TRIMOEA-TA&R, MO_RING_PSO_SCD, AND DN-NSGA-II USING PSP, AND COMPARISON BETWEEN IGDM AND PSP

In Table IV, we show the mean values of PSP [1] obtained by TriMOEA-TA&R, MO_Ring_PSO_SCD, and DN-NSGA-II on MMMOP1-6 and MMF1-8. '+' ('−') indicates that TriMOEA-TA&R shows significantly better (worse) performance in the comparison. '=' indicates that there is no significant difference between the compared results.

From Table IV, we can see that TriMOEA-TA&R significantly outperforms the other algorithms on most test problems. However, the result of PSP and IGDM in Table II in the main body of the paper are inconsistent on some test problems. For example, according to IGDM, TriMOEA-TA&R significantly performs better than MO_Ring_PSO_SCD on MMMOP2-A, and there is no significant difference between them on MMF1 and MMF3-5. On the other hand, according to PSP, MO_Ring_PSO_SCD achieves significantly better performance than TriMOEA-TA&R on MMMOP2-A, MMF1, MMF3, and MMF5, and TriMOEA-TA&R is the better one on MMF4.

There are two main reasons for the inconsistence between IGDM and PSP. The first is that PSP evaluates the uniformity of a solution set only in the decision space, since IGDX is a component of PSP. However, IGDM aims at evaluating the diversity performances both in the objective and the decision spaces. The second is that both IGDX and CR [1] in PSP measure the spread of a solution set in the decision space. Therefore, the spread of a solution set in the decision space dramatically affects the value of PSP.

Let us observe the difference between IGDM and PSP using a simple example. $PS_{\rm A}$, $PS_{\rm B}$, $PS_{\rm C}$, and $PS_{\rm D}$ are four PSs of MMMOP2-A. Their corresponding PFs in the objective space are $PF_{\rm A}$, $PF_{\rm B}$, $PF_{\rm C}$, and $PF_{\rm D}$, respectively. Fig. 19 shows the distributions of these PSs and PFs. $PS_{\rm A}$ is exactly the same as the PS shown in Fig. 3. Except the six leftmost solutions, the x_1 values of all the solutions in $PS_{\rm A}$ are larger than 0.95. $PS_{\rm A}$ is uniformly located on the PF in the objective space. The solutions in $PS_{\rm B}$ are uniformly distributed on each line in the decision space. However, the solutions are becoming denser with the increase of f_1 in the objective space. Except the leftmost solutions, the values of f_1 of all the solutions in $PF_{\rm B}$ are larger than 0.8. $PS_{\rm C}$ are the solutions in $PS_{\rm A}$ with the six leftmost solutions deleted. $PS_{\rm D}$ are the solutions in $PS_{\rm B}$ with the six rightmost solutions deleted. Then, all the solutions in $PS_{\rm C}$ ($PF_{\rm D}$) concentrate in a small region in the decision (objective) space.

TABLE V
RESULTS OF DIFFERENT METRICS

	$PS_{\rm A}$	$PS_{\rm B}$	$PS_{\rm C}$	$PS_{\rm D}$
IGDM	3.962E-03	1.669E-01	3.993E-03	3.553E-01
IGDX	2.258E-01	2.523E-03	4.521E-01	2.553E-03
MS	1.000E+00	1.000E+00	9.949E-01	3.970E-01
CR	1.000E+00	1.000E+00	3.662E-01	9.966E-01
PSP	4.428E+00	3.964E+02	8.100E-01	3.904E+02

Table V gives the results of IGDM, IGDX, MS [5], CR, and PSP of the four PSs in gray scale, where a darker tone corresponds to a worse value of each metric.

From Table V, we can see that both MS and CR of $PS_{\rm A}$ and $PS_{\rm B}$ are 1, since they cover both the whole true PF and PS. $PS_{\rm B}$ has a much better value of IGDX as well as PSP than $PS_{\rm A}$, because it is more uniform in the decision space. Conversely, the IGDM value of $PS_{\rm A}$ is better than $PS_{\rm B}$. Due to the low coverage of the true PS, $PS_{\rm C}$ has a poor value of IGDX and CR and thus an extremely poor value of PSP. However, its IGDM value is much better than those of $PS_{\rm B}$

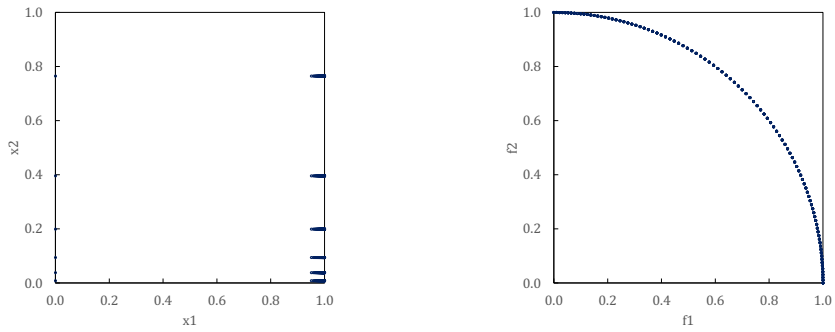

(a) PS_{A} (b) PF_{A}

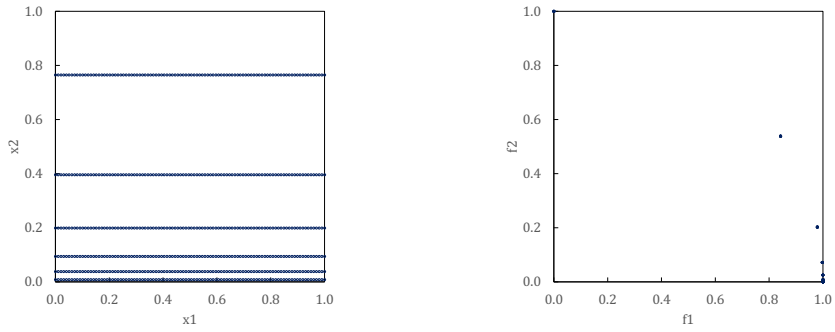

(c) PS_{B} (d) PF_{B}

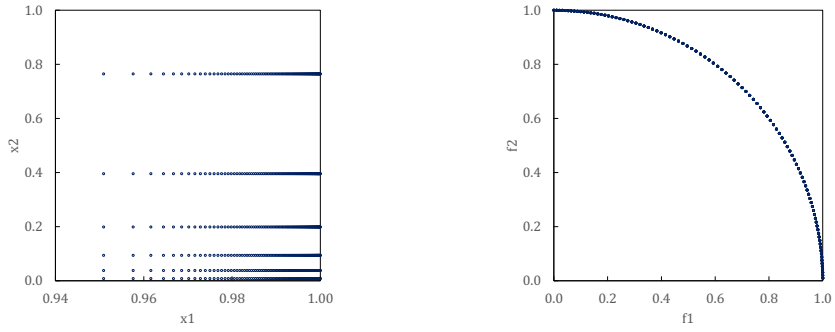

(e) PS_{C} (f) PF_{C}

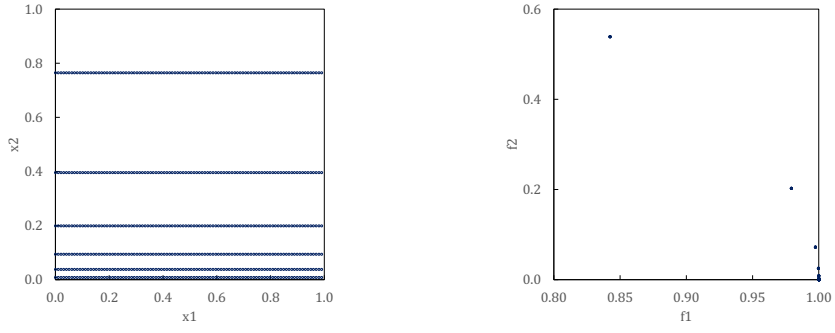

(g) PS_{D} (h) PF_{D}

Fig. 19. The distributions of PS_{A}, PS_{B}, PS_{C}, PS_{D}, and their corresponding PFs.

and PS_{D}, and its PF still shows a good coverage on the true PF according to MS. The IGDX, CR, and PSP values of PS_{D} are slightly worse than those of PS_{B}. However, its IGDM and MS values are the worst due to its poor distribution in the objective space.

We can observe from this example that the value of PSP is mainly dependent on the distribution of solutions in the decision space, especially the spread of solutions. This is why PSP behaves differently from IGDM.

VI. Computational Complexity Analysis of TriMOEA-TA&R

In each generation, the main difference between the proposed TriMOEA-TA&R and most existing MOEAs lies in the environmental selection strategy, where TriMOEA-TA&R adopts a two-archive based selection strategy. In the following, we analyze the computational complexity of this strategy.

Assume there is a population with its size of N to solve an optimization problem with M objectives and n decision variables, and the sizes of the convergence and the diversity archives are both equal to the population size. For the convergence archive, the complexity of calculating the convergence indicator and the distances in the decision space and sorting solutions in terms of the convergence indicator are $O\left(MN\right)$, $O\left(nN^2\right)$, and $O\left(N^2\right)$, respectively. Supposing that M and n are in the same order of magnitude, and they are smaller than N, the complexity of the selection strategy in the convergence archive is $O\left(MN^2\right)$. Similarly, for the diversity archive, the complexity of calculating the Pareto dominance relationship and the distances in the decision space and clustering in terms of the reference points are $O\left(MN^2\right)$, $O\left(nN^2\right)$, and $O\left(N^2\right)$. Thus the complexity of the selection strategy in the diversity archive is also $O\left(MN^2\right)$. In general, the overall complexity of the algorithm will be $O\left(MN^2\right)$, which is the same to that of most state-of-the-art MOEAs, e.g., NSGA-II [6]. Therefore, TriMOEA-TA&R is computationally efficient. In addition, as aforementioned in Subsection III.E in the main body of the paper, TriMOEA-TA&R would require a much smaller population than traditional MOEAs.

References

[1] C. Yue, B. Qu, and J. Liang, "A multi-objective particle swarm optimizer using ring topology for solving multimodal multi-objective problems," *IEEE Transactions on Evolutionary Computation*, 2017, Early Access.

[2] J. Liang, C. Yue, and B. Qu, "Multimodal multi-objective optimization: A preliminary study," in *2016 IEEE Congress on Evolutionary Computation (CEC)*. IEEE, 2016, pp. 2454–2461.

[3] D. A. Van Veldhuizen and G. B. Lamont, "On measuring multiobjective evolutionary algorithm performance," in *IEEE Congress on Evolutionary Computation*, vol. 1. IEEE, 2000, pp. 204–211.

[4] Y. Liu, D. Gong, J. Sun, and Y. Jin, "A many-objective evolutionary algorithm using a one-by-one selection strategy," *IEEE Transactions on Cybernetics*, vol. 47, no. 9, pp. 2689–2702, 2017.

[5] E. Zitzler, K. Deb, and L. Thiele, "Comparison of multiobjective evolutionary algorithms: Empirical results," *Evolutionary Computation*, vol. 8, no. 2, pp. 173–195, 2000.

[6] K. Deb, A. Pratap, S. Agarwal, and T. Meyarivan, "A fast and elitist multiobjective genetic algorithm: NSGA-II," *IEEE Transactions on Evolutionary Computation*, vol. 6, no. 2, pp. 182–197, 2002.